

A Virtual Reality Meditative Intervention Modulates Pain and the Pain Neuromatrix in Patients with Opioid Use Disorder

Mohammed M. Faraj,^{*} Nina M. Lipanski,[†] Austin Morales,[‡] Elimelech Goldberg,^{*,§} Martin H. Bluth, MD, PhD,^{*,§,|||} Hilary A. Marusak, PhD,^{‡,¶} and Mark K. Greenwald , PhD^{‡,||}

^{*}School of Medicine, Wayne State University, Detroit, Michigan; [†]Department of Biological Sciences, University of California, San Diego; [‡]Department of Psychiatry and Behavioral Neurosciences, Wayne State University; [§]Kids Kicking Cancer; [¶]Merrill Palmer Skillman Institute for Child and Family Development, Wayne State University; ^{||}Department of Pharmacy Practice, Wayne State University; ^{|||}Maimonides Medical Center, Brooklyn, New York, USA

Correspondence to: Mark K. Greenwald, PhD, Department of Psychiatry and Behavioral Neurosciences, Tolan Park Medical Building, 3901 Chrysler Service Drive, Suite 2A, Detroit, MI 48201, USA. Tel: +1 313 993 3965; Fax: +1 313 993 1372; E-mail: mgreen@med.wayne.edu.

Conflicts of interest: E.G. is founder and global director of Kids Kicking Cancer (KKC), a nonprofit organization that developed this martial arts intervention. M.B. is the global medical director of KKC. H.A.M. has received previous grant funding from KKC, and this research was funded by a subcontract from KKC (E.G.) to M.K.G. There are no other conflicts of interest to report.

Abstract

Objective. Standard of care for opioid use disorder (OUD) includes medication and counseling. However, there is an unmet need for complementary approaches to treat OUD patients coping with pain; furthermore, few studies have probed neurobiological features of pain or its management during OUD treatment. This preliminary study examines neurobiological and behavioral effects of a virtual reality-based meditative intervention in patients undergoing methadone maintenance treatment (MMT). **Design.** Prospective, non-blinded, single-arm, 12-week intervention with standardized assessments. **Setting.** Academic research laboratory affiliated with an on-site MMT clinic. **Methods.** Fifteen (11 female) MMT patients completed a virtual reality, therapist-guided meditative intervention that included breathing and relaxation exercisesessions were scheduled twice weekly. Assessments included functional magnetic resonance imaging (fMRI) of pain neuromatrix activation and connectivity (pre- and post-intervention), saliva cortisol and C-reactive protein (CRP) at baseline and weeks 4, 8 and 12; and self-reported pain and affective symptoms before and after each intervention session. **Results.** After each intervention session (relative to pre-session), ratings of pain, opioid craving, anxiety and depression (but not anger) decreased. Saliva cortisol (but not CRP) levels decreased from pre- to post-session. From pre- to post-intervention fMRI assessments, pain task-related left post-central gyrus (PCG) activation decreased. At baseline, PCG showed positive connectivity with other regions of the pain neuromatrix, but this pattern changed post-intervention. **Conclusions.** These preliminary findings demonstrate feasibility, therapeutic promise, and brain basis of a meditative intervention for OUD patients undergoing MMT.

Key Words: Methadone; Meditation; fMRI; Pain Neuromatrix; Postcentral Gyrus; Craving; Cortisol

Introduction

Opioid misuse, overdose, and opioid use disorder (OUD) constitute a public health emergency that is persistent [1] and projected to escalate [2]. In 2018, about 2 million individuals in the US had an OUD [3], which is associated with a high mortality rate (± 130 daily deaths in the US), comorbid psychiatric disorders (e.g., anxiety), and other poor health outcomes [4]. Further interventions are

needed to reduce the impact of opioid misuse, OUD, and overdose.

Chronic pain affects >100 million individuals in the United States and opioids prescribed to treat pain can increase risks of misuse, physiological dependence, and OUD [5]. Previous research indicates 64.4% of OUD patients report chronic pain [6], which may occasion relapse [7], reduce adherence to OUD treatment, and reduce quality of life [8]. Additionally, prevalence of OUD among patients with chronic pain is 34.9% [9]. Standard

of care for OUD includes medication, such as methadone maintenance therapy (MMT), and counseling. Given adverse effects of chronic pain among patients with OUD, there is an unmet need for complementary approaches to assist OUD patients with pain.

One potential complementary approach for reducing pain in OUD is mindfulness-based therapies (e.g., breathing, meditation). Mindfulness is the practice of focusing on the present moment to improve control over one's own sensations, feelings, and thoughts. Mindfulness approaches have been shown to reduce pain intensity and pain-related psychological consequences, and to improve functional status and quality of life [10]. Findings from studies in healthy populations suggest that meditative interventions can mitigate pain, independent of the endogenous opioid system [11, 12]. Previous controlled studies report that mindfulness meditation can reduce self-reported pain in patients with chronic pain conditions [13] and in opioid-using chronic pain patients [14].

Although meditation-based therapies show promise for reducing pain in individuals with OUD and other groups, neurobiological mechanisms underlying these analgesic effects remain unclear. The "pain neuromatrix" is a core set of brain regions recruited when an individual experiences physical pain [15]. The pain neuromatrix includes primary nociceptive processing regions including the thalamus, anterior insula, caudate, postcentral gyrus (PCG), anterior midcingulate cortex (aMCC), and posterior cingulate cortex (PCC). The pain neuromatrix also includes regions involved in sensory/affective appraisal, for example, dorsolateral prefrontal cortex [16, 17], polymodal regions that are not specifically related to nociception such as the ACC, and primary and secondary somatosensory cortices [18]. Relevant to the present study, regions of the pain neuromatrix are engaged when one person watches another person experiencing physical pain [19]. Importantly, meditation has been shown to modulate activity and connectivity within the pain neuromatrix [20]. Prior studies reported lower prefrontal activation and higher insula and PCG activation to pain-related processing following a meditation intervention [21, 22]. The pain neuromatrix has also been implicated in the development and maintenance of OUD [4]. Thus, interventions that target the pain neuromatrix may be beneficial for addressing mechanisms involved in pain and OUD etiology.

This pilot study examined neurobiological and behavioral effects of a novel meditative intervention in OUD patients undergoing MMT. We hypothesized that participation in this meditative intervention would lead to less task-induced activation and resting-state connectivity of the pain neuromatrix; lower saliva levels of cortisol (index of hypothalamic-pituitary-adrenal [HPA] axis response) and C-reactive protein ([CRP], inflammatory

biomarker); and less self-reported pain, opioid craving, and affective symptoms.

Methods

Setting

We recruited participants enrolled in an urban, academic-affiliated MMT program. This not-for-profit, evidence-based practice, treatment research-oriented clinic (unique in the Detroit metropolitan catchment area) had a census of about 150 patients at the time of this study. Services are primarily funded by Medicaid or Block grants. The majority of patients in this clinic are African American, have comorbid medical and psychiatric conditions, and report prior (often multiple) OUD treatment episodes. Most patients in this clinic are maintained on methadone, and a few on buprenorphine.

Participants

Participants were enrolled and completed the study from October 8, 2018, through September 20, 2019. All participants were ≥ 18 years old, met criteria for OUD, and were stabilized on their methadone dose for >1 month before screening. We excluded individuals who were pregnant or lactating, had a current severe Axis I psychiatric disorder (e.g., psychosis, bipolar), past-year suicidal ideation/attempt, and contraindications to the intervention (e.g., cognitive or physical disability, unwillingness to undergo the procedures) or magnetic resonance imaging (MRI). Demographic and substance use history data were obtained from patients' clinical charts. All participants provided informed consent following approvals from Wayne State University and State of Michigan IRBs. The study was registered at ClinicalTrials.gov (NCT03595007).

Study Design

This pilot study was a single-arm, 12-week virtual reality (VR) meditative intervention. Upon enrollment, we obtained pre-intervention baseline measures of chronic pain, affective distress (i.e., anxiety, depression), emotion regulation and self-efficacy. Intervention sessions were scheduled twice weekly on methadone clinic attendance days. Before and after each session, participants rated their pain and other symptom severity using visual analog scales (VASs). Saliva samples were collected before and after four sessions (baseline and weeks 4, 8, and 12). Two MRI scans were performed, before (baseline) and after the 12-week intervention, to measure pain neuromatrix activity and connectivity. Participants were compensated for completing research visits using electronic payments.

Pre-Intervention Baseline Measures

Chronic pain severity and functional interference was measured using the Brief Pain Inventory (BPI) [23], which

has been validated in MMT patients [24]. Participants also completed the Beck Depression Inventory-II (BDI-II) [25, 26], which measures past 2-week depression symptoms; State-Trait Anxiety Inventory (STAI) [27], which differentiates state anxiety from more chronic trait anxiety; Distress Tolerance Scale [28], which measures the ability to remain drug abstinent in the face of difficulties [29, 30]; Perceived Stress Scale [31], which measures the degree to which the subject views past-month situations in his/her life as stressful; Difficulties with Emotion Regulation Scale [32], which measures non-acceptance of emotional responses, difficulties in engaging in goal-directed behavior, impulse control difficulties, lack of emotional awareness, limited access to emotion regulation strategies, and lack of emotional clarity; and Alcohol and Drug Use Self-Efficacy Scale [33], which assesses self-efficacy and responses to high-risk situations that can precipitate substance use. Items are grouped into negative affect, social positive withdrawal/urges, and physical/other concerns; subjects indicate how “tempted” and “confident” they would be in each situation, yielding two scores.

Virtual reality Meditative Intervention

Meditative interventions, including martial arts, yoga, and mindfulness-based approaches, are a promising approach for attenuating pain [34]. Martial arts, in particular, as a therapeutic model leverages the popular notion that associates martial artists as being powerful. This is an attractive theme to children diagnosed with, and being treated for, life-threatening illness [35, 36]. It may also resonate with patients exhibiting diminished self-regulation and perceived loss of self-agency including substance use disorders [37]. Although hundreds of martial arts styles are taught worldwide (e.g., Tai Chi, Chi Gung, Karate), limb movements, controlled breathing and mental focus (e.g., meditation) are unifying factors. The approach described here differs from other modalities of meditation, mindfulness, and fighting-oriented martial arts, as it blends key elements from such modalities, uses VR, and is individually tailored [35, 36].

Using narration and VR technology to teach and engage the participant, the intervention coordinates physical (arms, hands, upper body) movements with a specific breathing technique, and meditative exercises (which are neither distracting nor dissociative) to vividly imagine and act as a powerful martial arts “warrior” who must face down his/her internal personal struggles. The physical movement/breathing sequence uses the Breath Brake[®], which involves three cycles of inhaling (3-second duration) while hands are raised, palms up from waist to shoulders, breath-holding (3-second duration) while hands are rotated to palms facing down, and exhaling (3-second duration) while palms are lowered from shoulders to waist, each time envisioning “breathing in the light and breathing out the darkness.” This breathing process

is accompanied by upward body movement during inhalation, lowering the body while relaxing muscles during exhalation, toward propagating a gentle, fluid wavelike motion throughout the cycle. At the end of exhalation, the participant forcefully expels the breath, which engages vagal responses shown beneficial in many disease states [38, 39]. This motor sequence decouples the automatic breathing rhythm into distinct quanta, and is intended to promote active engagement and control, in contrast to being passively receptive in conventional therapy.

The 12-week intervention consisted of 30-min sessions scheduled twice-weekly. Participants completed 16–24 sessions ($M = 21.7$, $SD = 2.1$). Sessions occurred in a private, soundproof room. The trained therapist worked 1:1 with the participant to teach VR-assisted martial arts-based movements, breathing and meditative techniques. Participants learned the Kids Kicking Cancer (KKC; www.kidskickingcancer.org) mantra “Power. Peace. Purpose.” and practiced the Breath Brake[®] [35, 36] as described above. The VR platform used a Windows Mixed Reality headset attached to a gaming laptop with an advanced processor and video card that assured a seamless 360° immersive audio and video experience. During sessions, the therapist first asked the participant to recount past-week events, whether they used the Breath Brake[®] or other techniques for stressful life events, and reminded them to use the Breath Brake[®] the next time a stressful event arose. The participant then underwent a 15-minute VR-guided meditation. The first meditation introduces the KKC program, presented with eight KKC children. Author EG explains to the participant that the children have less pain when they know others are learning from them. The participant is put in the position of helping children with cancer by doing the Breath Brake[®], and that the therapist will report their progress to the children. The next scene takes place with the children as avatars teaching the participant how to do a Breath Brake[®]. The children also inform the participant that the greatest opponent to any martial artist lies within oneself. The children explain that parts of our brains can turn into a beast that can seek to destroy us. In the next scene the participant is brought back, through the optic nerve into his/her brain, to face the beast. The limbic system twirls and turns into a beast, which demands the participant get rid of the children. “You love me. I am everything to you.” The child appears next to the beast and reminds the participant to use his/her breath to destroy the beast. “Your beast is a liar,” the child informs the participant. As the participant breathes in, the VR fills with a powerful light. As the participant exhales, he/she can see his/her breath as smoke that makes holes in the beast. The beast begins to shrink. The beast is fully washed away in the next section during a waterfall meditation. The participant is warned the beast will return but that when we continue to use our light to defeat it, the beast will no longer have the power to destroy us. Participants were

also issued a mobile phone-based application for their own use at home. Using the voice of a child cancer patient in the KKC program, the software issued reminders to the participant, encouraging him/her to take Breath Brakes[®] at scheduled intervals (default was every 2 hours, but this could be adjusted by the participant).

VAS ratings

Before and after each intervention session, the participant rated his/her momentary level of “pain,” “opioid craving,” “anxiety,” “anger,” and “depression” using a VAS (0–10; 0 = not at all; 10 = extremely).

Saliva Samples

At pre-intervention baseline and weeks 4, 8, and 12, pre- and post-session saliva samples were collected using a non-stimulated, passive drool method, collected with a salivette held under the tongue for 3 min. Samples were frozen at -20°C prior to analysis.

MRI Scanning

Scan Parameters

MRI data were collected before and after the 12-week intervention using a single Siemens 3T MAGNETOM Verio system (Siemens, Erlangen, Germany) equipped with a 32-channel head coil. BOLD fMRI data were acquired using a multi-echo T2*-weighted, multiband-accelerated EPI sequence with 51 near-axial 64×65 slices (voxel size 2.9-mm isotropic; TR = 1500-ms; TEs = 15, 31, 46-ms; flip angle = 83, FOV = 186×186 ; GRAPPA factor = 2, multi-band factor = 2). High-resolution structural (anatomical) images were acquired each session using a T1-weighted MP-RAGE sequence (voxel size: $0.7 \times 0.7 \times 1.3$ -mm; TR = 1680-ms; TE = 3.51-ms; flip angle = 9; FOV = 256×256 ; 128 slices; 1.34-mm slice thickness).

Functional Tasks

During fMRI scans, participants completed a 10-minute resting-state task. They were instructed to remain still with eyes closed during a functional localizer task that reliably isolates neural activity in the pain neuromatrix without inducing physical pain [19]. This task involves passively viewing a 5-minute 36-second video clip from the animated short film “Partly Cloudy” (Pixar Animation Studios). The movie clip includes events that evoke mental states and physical sensations of characters, including the character undergoing a physically painful event (e.g., electrocuted by an electric eel). In addition to pain-related events, other movie events were coded as non-pain conditions: control (e.g., no character-related events), social (characters interacting), and mentalizing (e.g., viewer is led to think about the character’s thoughts, such as when a character falsely believes he has been abandoned by his companion). Due to technical problems, post-intervention data were missing for two

participants for the pain task and for two participants for the resting-state task.

Data analysis

VAS Scores

To account for missing data, VAS responses (pain, opioid craving, anxiety, anger, depression) were averaged across protocol weeks to create four bins (i.e., weeks 1–3, 4–6, 7–9, 10–12), separately for pre- and post-session scores. Parallel session (pre/post) \times bin repeated-measures ANOVAs were conducted for each VAS score in IBM SPSS v.26. Follow-up *t*-tests were conducted following significant main effects or interactions, and all results were considered significant at $P < .05$ (two-tailed). Greenhouse-Geisser correction was used for sphericity violations.

Cortisol and C-Reactive Protein (CRP)

Saliva samples were analyzed by Salimetrics LLC (State College, PA) using radioimmunoassays for cortisol and CRP levels. To reduce skewness of distributions, raw cortisol and CRP values were \log_{10} transformed prior to parallel session (pre/post) \times week (baseline and weeks 4, 8, 12) repeated-measures ANOVAs in SPSS. Follow-up *t*-tests were conducted following significant main effects or interactions, and all results were considered significant at $P < .05$ (two-tailed).

fMRI Preprocessing

Preprocessing and denoising steps were performed for BOLD fMRI data (pain neuromatrix task, resting-state task) using multi-echo independent components analysis (ME-ICA) software (v.2.5; <https://github.com/ME-ICA/me-ica>) [40]. ME-ICA leverages quantitative T2* decay measures to separate BOLD from non-BOLD (e.g., head motion) signals using ICA. This step circumvents relatively arbitrary preprocessing steps and reduces signal dropout by acquiring an early echo (15-ms) and optimal combination of echoes. Multi-echo imaging can increase signal-to-noise ratio and fMRI effect sizes compared to standard denoising approaches, which is useful for pilot studies [41]. Preprocessing steps in ME-ICA include coregistration to anatomical images and normalization to Montreal Neurologic Institute (MNI) standard space. fMRI scan quality was assessed using framewise displacement (FD), a measure of frame-to-frame movement [42]. Mean FD in the unprocessed data for the pain neuromatrix task was 0.37 mm (SD = 0.25) at baseline and 0.45 mm (SD = 0.3) at post-intervention. For the resting-state task, raw mean FD was 0.33 mm (SD = 0.23) at baseline, and 0.4 mm (SD = 0.26) at post-intervention. ME-ICA preprocessing and denoising for task and resting-state data significantly reduced head motion compared to the raw data ($ts > 10$, $ps < 0.001$).

Pain Neuromatrix Task

The optimally combined and denoised task BOLD fMRI time-series data sets were submitted to Statistical Parametric Mapping software (SPM8; <https://www.fil.ion.ucl.ac.uk/spm/software/spm8/>) for analysis. Data were modeled using a general linear model (GLM), following prior work [19]. First-level models included condition regressors associated with the four event types in the movie (pain, control, social, and mentalizing). These events were modeled as boxcar functions and convolved with a canonical hemodynamic response function.

Pain neuromatrix activation was isolated using the contrast, pain > mentalizing. Group-level analyses were conducted using complementary region-of-interest (ROI) and whole-brain exploratory approaches. ROI and whole-brain analyses both used well-established approaches to correct for multiple tests (i.e., GLM across all brain voxels). The ROI approach restricts the search space to a priori ROIs implicated in neural processes of interest (here, pain-related processing), then controls for multiple comparisons within that search space by extracting single-value summary measures (e.g., weighted mean neural activation; 40]. The whole-brain approach applied cluster correction, a common correction method in fMRI analyses, which relies on the fact that voxels are not completely independent [43]. This approach controls familywise error (FWE) rate. We also used Monte Carlo simulations to identify a minimum cluster size (i.e., minimum number of contiguous voxels that are significant) at a conservative voxel-wise threshold ($P < 0.001$), following prior recommendations [43].

For the ROI approach, we analyzed five pain neuromatrix ROIs from Jacoby et al. [19] using the same task in healthy individuals and the same contrast. We created spherical ROIs (12-mm radii) centered on peak activation (pain > mentalizing) for the aMCC, right and left anterior insula (AI), right and left PCG (Figure 1). For each participant, we extracted and analyzed from baseline and post-intervention scans the first principal component of the pain > mentalizing activation in each ROI (β -estimates). First, we conducted one-sample t -tests to evaluate whether activation in each ROI significantly differed from 0 at baseline and post-intervention scans, separately. Then, we applied paired-sample t -tests to assess activation change in each ROI between baseline and post-intervention. Pearson bivariate correlations were applied to test whether baseline pain severity or functional interference (BPI), modulated pain-related activity in pain neuromatrix ROIs at baseline or post-intervention. Exploratory correlations were conducted to examine whether saliva cortisol or CRP levels were related to pain-related neuromatrix activation. Within SPM8, a complementary whole-brain FWE corrected threshold $p_{FWE} < 0.05$ was applied for exploratory purposes, to evaluate overall patterns of pain-related activation separately at baseline and post-intervention (one-sample t -

tests), and for changes in activation between baseline and post-intervention (paired-samples t -tests). The whole-brain corrected threshold was determined using AFNI's (version AFNI_19.2.24: linux_openmp_64) 3dFWHMx (compile date: September 14, 2019, https://afni.nimh.nih.gov/pub/dist/doc/program_help/3dFWHMx.html) and 3dClustSim (voxelwise $P < .001$; cluster threshold = 5 voxels). This approach accurately models the spatial autocorrelation inherent in fMRI data [44]. All xyz coordinates provided in this report are in MNI convention.

Resting-State Connectivity

We also examined resting-state functional connectivity of the pain neuromatrix. Resting-state functional connectivity is based on measurement of spontaneous fluctuations in fMRI signals and is commonly used to probe stable patterns of brain network organization at rest, or independent of task-specific constraints. Prior research demonstrates that resting-state connectivity patterns correspond highly with brain activation and connectivity patterns observed during tasks [45–47], are reliable across contexts (e.g., at rest or across various tasks; 45], vary between neurotypical and abnormal individuals, and correspond with measures of chronic pain or acute pain sensitivity [48, 49]. These findings suggest resting-state patterns reflect underlying synaptic efficacies in brain networks and thus correspond to a canonical or “intrinsic” state of functional brain organization [50]. Here, we focused on resting-state connectivity of pain neuromatrix ROIs that showed significant pain-task activation, that is, left and right PCG (see *Results*). These analyses were performed using multi-echo independent components regression (ME-ICR) [40]. Rather than using the optimally combined BOLD time series, ME-ICR uses the independent BOLD components derived from ME-ICA as the effective degrees of freedom for each subject to control for false positives [40]. BOLD components were submitted to the MATLAB-based program CONN software v.19.c [51] for seed-based connectivity of left and right PCG ROIs using Pearson bivariate correlation. The correlation was calculated between the extracted vector of weights for each ROI and every other brain voxel. Fisher's r -to- Z transform was then applied to the resulting correlation image. At the group level, we first performed one-sample t -tests to examine patterns of connectivity for left and right PCG at baseline and post-intervention. Next, paired-sample t -tests were used to examine changes in left and right PCG connectivity between baseline and post-intervention. Finally, regression was used to test whether baseline pain severity or functional interference was associated with left and right PCG connectivity at baseline or post-intervention, or change in connectivity between baseline and post-intervention. Results were considered significant using a whole-brain corrected threshold determined using 3dFWHMx and 3dClustSim (voxelwise $P < .001$; cluster

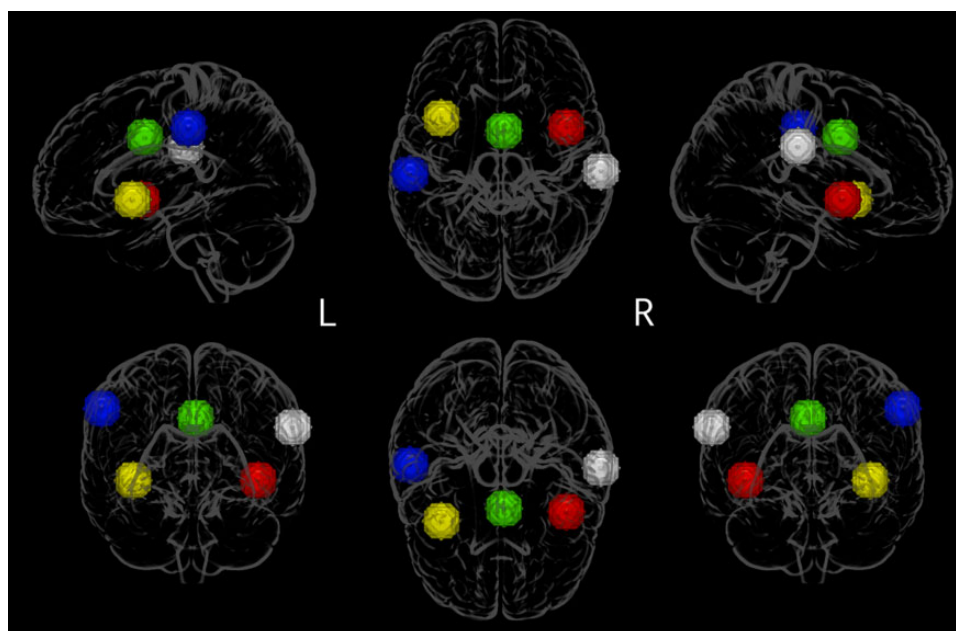


Figure 1. Pain neuromatrix regions of interest (ROIs) from Jacoby et al. (2016). Left = sagittal view; right: coronal view from front. Red: right anterior insula; yellow: left anterior insula; green: anterior middle cingulate cortex; white: right postcentral gyrus; blue: left postcentral gyrus. ROIs defined using 12 mm spheres around pain neuromatrix peaks reported in Jacoby et al. (2016).

threshold = 5 voxels). Resulting test statistics are given as Z-scores, which refers to the z statistic at the peak coordinate location. For baseline connectivity patterns, the Z-score was computed from the *t*- and *P* values derived from the group-level one-sample *t*-test. Higher Z-scores represent stronger connectivity between brain regions. For pre-post changes in connectivity, the Z-score was computed from the *t*- and *P* values derived from the group-level paired-samples *t*-test. Higher Z-scores represent greater pre-post intervention changes in functional connectivity between regions.

Results

Baseline Characteristics

Fifteen participants completed the study (Table 1). The sample was primarily female, balanced on race and injection drug use; several participants had co-occurring substance use or mental health problems. Participants were chronic opioid users (primarily heroin) and were receiving an average methadone dose of about 95 mg at entry into the study.

Baseline pain severity ranged from 0 to 32, and baseline pain functional interference ranged from 0 to 59 (Table 1). Location of the most severe chronic pain varied across participants; however, most patients (93.3%) reported low-back pain. Maximum pain in the past 24-hr was 4.8 of 10 (SD = 3.8), with 10 being “the most extreme pain imaginable”. BPI pain severity and functional interference scores were positively correlated, $r(15)=0.69$, $P = .004$, but not associated with age, sex, race, years of education, state anxiety or depression

scores, methadone dose during the intervention (max, min, average, modal), nor baseline scores for Alcohol and Drug Use Self-Efficacy, or Difficulties in Emotion Regulation, $ps>0.05$.

Session and Week-Related Changes in VAS Scores

Session (pre/post) \times week (binned) repeated-measures ANOVA demonstrated a significant main effect of session for VAS pain scores: post-session levels were lower than pre-session levels ($F(1, 42)=5.04$, $P = .042$, $\eta p^2=0.265$; Figure 2A). There was also a significant main effect of session on opioid craving, anxiety, and depression scores: post-session levels were lower than pre-session levels ($ps<0.05$). For craving, there was also an effect of week, $F(1.85, 25.84)=4.59$, $P = .022$, such that craving decreased from weeks 1–6, increased from weeks 7–9, and decreased again from weeks 10–12 ($ps<0.05$). There were no significant main effects or interactions for anger ($ps>0.05$).

Session and Week-Related Changes in Salivary Cortisol and CRP

Session (pre/post) \times week repeated-measures ANOVA for saliva cortisol and CRP showed a significant main effect of session on cortisol, $F(1, 14)=22.69$, $P < .001$, $\eta p^2=0.62$ (Figure 2B). Post-session cortisol levels were lower than pre-session. There were no significant main effects or interactions for CRP ($ps>0.05$).

Table 1. Participant demographic characteristics and substance use history (n = 15)

Variable	n	%
Sex		
Female	11	73
Male	4	27
Age		
19–29 years	2	13.33
30–49 years	5	33.33
50+ years	8	53.33
Race		
White	8	53.3
Black	7	46.7
Disabled	2	13.3
Injection opioid use	7	46.7
Marital status		
Single/widowed/divorced	11	73.3
Married or cohabitating	4	26.7
Unemployed	13	86.7
Comorbid substance use disorder	8	53.3
Cocaine	5	33.3
Benzodiazepines	2	13.3
Comorbid current mental health diagnosis	7	46.7
Major depressive disorder	5	33.3
Anxiety disorder	2	13.3
	M	SD
Average methadone dose (mg)	94.9	30.6
Years of opioid use	22.6	16.4
Years of education	11.4	1.6
Pain severity (BPI)	15.2	10.0
Pain functional interference (BPI)	20.9	19.5
State anxiety (STAI-S; range, 0–80)	49.3	2.7
Depression symptoms (BDI-II; range, 0–63)	12.5	10.1
Distress tolerance (DTS; range, 0–75)	58.7	11.1
Perceived stress (PSS; range, 0–40)	23.2	6.2
Difficulties with emotion regulation (DERS; range, 0–180)	82.1	10.6
Alcohol and drug use self-efficacy (ADUSE); tempted (range, 0–50)	39.7	19.4
Alcohol and drug use self-efficacy (ADUSE); confident (range, 0–50)	71.5	25.2
Baseline pain (VAS; range, 0–10)	6.6	2.4
Baseline opioid craving (VAS; range, 0–10)	5.2	1.3
Baseline anxiety (VAS; range, 0–10)	8.2	2.6
Baseline anger (VAS; range, 0–10)	3.8	0.8
Baseline depression (VAS; range, 0–10)	4.0	1.13

Pain severity and functional interference measured using the Brief Pain Inventory (BPI); state anxiety measured using the State-Trait Anxiety Inventory (STAI-S); depressive symptoms measured using the Beck Depression Inventory-II (BDI-II); VAS, visual analog scale. DTS data missing for one participant; PSS data missing for two participants.

Pain Neuromatrix Activation

At baseline, left and right PCG showed significantly positive activation, $t(14)=4.69$, $P < .001$, and $t(14)=2.88$, $P = .012$, respectively (Figure 3A). No other ROIs showed activation that significantly differed from zero at baseline or post-intervention ($ps>0.05$). Activity in left PCG significantly decreased from baseline to post-intervention, $t(12)=2.61$, $P = .023$ (Figure 3B). No other ROIs showed a significant change in activation from baseline to post-intervention ($ps>0.05$). No regions showed significant activation at baseline or post-intervention, or

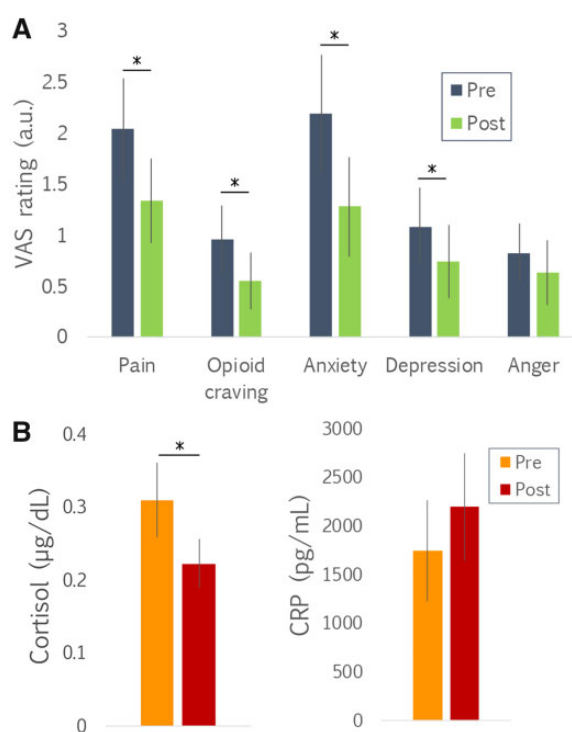


Figure 2. (A) Significant pre-post session reductions in self-ratings of pain, opioid craving, anxiety, and depression. (B) Significant pre-post session reduction in salivary cortisol. Raw values for cortisol and C-reactive protein (CRP) are given but analyses performed on \log_{10} transformed values. * $P < .05$.

between baseline and post-intervention, at the exploratory corrected whole-brain threshold $pFWE < 0.05$.

Higher baseline pain functional interference was associated with higher pain-related activation only in left PCG at baseline, $r(15)=0.56$, $P = .03$ (Figure 3C). Pain severity was not associated with activation in any ROI at baseline or post-intervention.

We also conducted exploratory correlation analyses to examine whether saliva biomarkers were related to task activation. Higher baseline pre-session cortisol was associated with higher pain-related activation in left PCG at baseline, $r(15)=0.591$, $P = .02$. Higher baseline pre- and post-session cortisol levels were associated with higher pain-related activation in right and left AI at post-intervention ($rs = 0.56-0.7$, $ps < 0.05$). Higher baseline pre-session CRP was associated with higher pain-related activation in the right PCG at baseline, $r(14)=0.557$, $P = .037$, and higher baseline post-session CRP was associated with higher pain-related activation in the right PCG ($r(12)=0.652$, $P = .021$) and left AI ($r(12)=0.640$, $P = .025$) at post-intervention. However, none of the above results survived correction for multiple comparisons.

Pain Neuromatrix Functional Connectivity

At baseline, PCG was positively connected with other pain neuromatrix regions including dorsal posterior insula, inferior frontal gyrus, precentral gyrus, middle frontal gyrus, superior temporal gyrus, inferior parietal

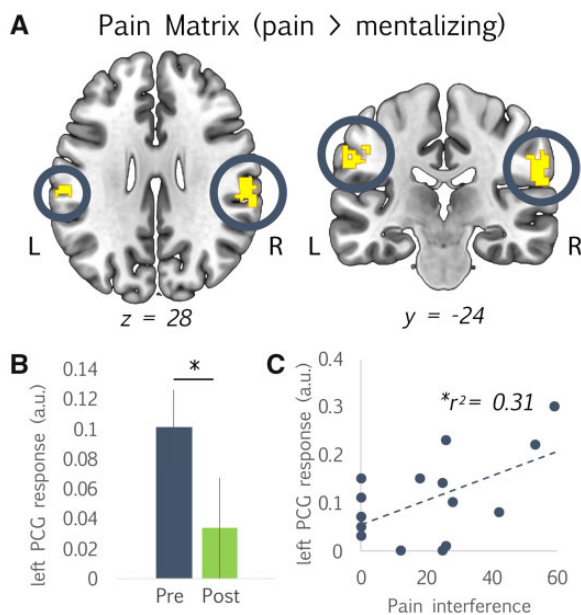


Figure 3. (A) Activation in the left and right postcentral gyrus (PCG) regions of interest (ROIs) during the Partly Cloudy task for the contrast pain > mentalizing during pre-intervention baseline. Image thresholded at $P < .05$ uncorrected, masked within the five pain neuromatrix ROIs (see Figure 1) for display purposes. (B) Reduction in pain-related activity in the left PCG at post-intervention, compared to pre-intervention baseline (contrast: pain > mentalizing), $*P < .05$. (C) Higher self-reported pain functional interference at baseline is associated with higher pain-related activation in the left PCG (contrast: pain > mentalizing) at baseline.

lobe, and cerebellum (Table 2). At baseline, PCG showed negative connectivity with posterior cingulate cortex (PCC) and with clusters in the superior temporal gyrus and middle frontal gyrus that differed from those with positive connectivity. These patterns are consistent with prior studies showing positive connectivity between the PCG and other regions of the pain neuromatrix at rest and during noxious stimulation (e.g., [48, 49]).

Next, we examined changes in PCG connectivity between baseline and post-intervention (Table 2). PCG and other pain neuromatrix regions exhibited lower connectivity strength (in terms of magnitude and spatial extent) at post-intervention compared to baseline, including the superior temporal gyrus, inferior frontal gyrus, caudate, and aMCC (Figure 4). In contrast, PCG connectivity with inferior parietal lobe and contralateral PCG was higher at post-intervention compared to baseline.

Next, we tested whether baseline pain severity and functional interference was associated with PCG connectivity at baseline and post-intervention (Table 3). Higher pain severity at baseline was associated with stronger PCG connectivity with cerebellum and medial frontal gyrus, and lower PCG connectivity with precentral gyrus and superior frontal gyrus at baseline. Pain interference was not associated with PCG connectivity at baseline. Higher baseline pain severity was associated with

stronger PCG connectivity with middle temporal gyrus and inferior parietal lobe, and lower PCG connectivity with occipital lobe and medial inferior parietal lobe at post-intervention. Higher baseline functional interference was associated with stronger PCG connectivity with inferior parietal lobe and inferior temporal lobe, and lower PCG connectivity with a lateral region of inferior parietal lobe and precentral gyrus at post-intervention.

Finally, we tested whether baseline pain severity or interference was associated with changes in PCG connectivity between baseline and post-intervention (Table 3). Higher pain severity at baseline was associated with lower connectivity of PCG with the superior parietal lobe, cerebellum, and PCC from baseline to post-intervention (Figure 5, upper row), and with stronger PCG connectivity with middle frontal gyrus, contralateral PCG, hippocampus, and a separate cluster in the cerebellum. Higher pain interference at baseline was associated with decreased PCG connectivity with superior parietal lobe and increased PCG connectivity with inferior parietal lobe, superior temporal gyrus, posterior PCG, and brainstem from baseline to post-intervention (Figure 5, lower row).

Discussion

This pilot investigation demonstrates the feasibility, therapeutic promise, and brain basis of a 12-week meditative approach for OUD patients undergoing MMT. We found reductions in self-reported pain, opioid craving, anxiety, depression, and saliva cortisol in OUD patients after treatment sessions. Further, pain task-related activation in a key region of the pain neuromatrix—the PCG—decreased from pre- to post-intervention. At baseline, the PCG showed positive resting-state connectivity with other regions of the pain neuromatrix, but this pattern changed post-treatment. Baseline pain severity scores were associated with PCG connectivity both at pre- and post-treatment, and with the change from pre- to post-treatment. Our preliminary findings that this intervention can reduce self-reported pain and modulate the pain neuromatrix suggest a promising complementary approach to assist OUD patients burdened with pain.

On average, OUD patients in our sample reported substantial pain (4.8 of 10), consistent with previous findings that many OUD patients endorse chronic pain. Higher pain levels have been associated with worse outcomes among patients with substance use disorders, including relapse and reduced quality of life [8]. Here, we observed that a meditative intervention with relaxation exercises can reduce pain, anxiety, depression, and opioid craving among OUD patients on MMT. Notably, we found that initial decreases in craving rebounded midway through treatment, then decreased again; reasons for these changes remain unclear but could be related to temporary setbacks that are normal during the course of MMT. This pattern highlights the clinical importance of

Table 2. Resting-state functional connectivity results for left and right postcentral gyrus (PCG) at pre-intervention baseline, and from pre- to post-intervention

Contrast Seed	Direction	Target Region	Brodmann Area	x	y	z	Cluster Extent	Z-Score
All participants: Functional connectivity at baseline (i.e., pre-intervention)								
Left PCG	Positive	Left PCG	2	-58	-32	44	168	3.85
		Left inferior parietal lobe	40	-42	-36	44	43	3.76
		Right inferior parietal lobe	40	60	-26	26	22	3.51
		Left PCG	3	-44	-26	40	14	3.71
		Left PCG	40	-62	-24	20	14	3.56
		Left inferior parietal lobe	2	-52	-28	34	12	3.27
		Left inferior frontal gyrus	9	-50	6	14	12	3.91
		Right inferior parietal lobe	40	60	-34	40	10	3.51
		Left inferior parietal lobe	2	-52	-38	40	10	3.41
		Left cerebellum (anterior lobe)	N/A	-32	-44	-32	8	3.15
		Left PCG	40	-52	-32	52	8	3.47
		Left cerebellum (anterior lobe)	N/A	-18	-50	-32	8	3.43
		Left inferior frontal gyrus	44	-58	8	22	8	3.18
		Left middle frontal gyrus	9	-52	12	34	6	3.18
		Left precentral gyrus	9	-52	2	38	6	3.53
Right PCG	Positive	Right inferior parietal lobe	40	66	-34	22	169	3.92
		Right PCG	3	60	-26	44	12	3.50
		Left PCG	40	-62	-28	20	11	3.71
		Left inferior parietal lobe	1	-62	-26	-26	9	3.59
		Right brainstem	N/A	8	-32	-52	8	3.13
		Right middle temporal gyrus	22	48	-58	2	8	3.43
		Left inferior parietal lobe	40	-58	-28	34	6	3.27
Left dorsal posterior insula	13	-42	-6	-2	5	3.44		
Right PCG	Negative	Left middle frontal gyrus	9	-37	22	40	12	3.45
		Right frontal lobe	24	20	2	28	8	3.13
Left PCG	Negative	Right superior temporal gyrus	22	48	-18	2	8	3.22
		Right posterior cingulate cortex	29	8	-58	8	8	3.48
All participants: Change in functional connectivity from pre- to post-intervention								
Left PCG	Pre > Post	Right superior temporal gyrus	38	34	8	-38	8	3.46
		Right inferior frontal gyrus	47	54	22	2	8	3.31
Right PCG	Pre > Post	Left caudate	N/A	-18	-18	22	8	3.46
		Left anterior middle cingulate cortex	24	-6	8	28	8	3.15
Left PCG	Post > Pre	Left inferior parietal lobe	40	-52	-28	48	216	3.97
		Right PCG	2	60	-32	40	8	3.09
Right PCG	Post > Pre	Right PCG	1	66	-20	32	266	4.18
		Left PCG	40	-62	-14	20	5	3.23

All reported results are significant at the whole-brain corrected threshold (familywise error corrected using Monte Carlo simulations; voxel-wise threshold $P < .001$ and cluster-level correction (cluster minimum = 5 voxels). Cluster extent refers to the number of contiguous voxels in a cluster and the minimum cluster size was determined to be 5 voxels. Coordinates (x, y, z) refer to the anatomical location in 3D brain space, reported in MNI convention, at the peak maximally activated voxel within the cluster. Anatomical location of the peak location is reported using Brodmann areas. Note that separate target regions can have separate significant clusters within the same target region, particularly for anatomically large cortical regions. Test statistic given as a Z-score, which refers to the z statistic at the peak coordinate location. For baseline connectivity patterns, the Z-score was computed from the t - and P values derived from the group-level one-sample t -test. Higher Z-scores represent stronger connectivity between brain regions. For pre-post changes in connectivity, the Z-score was computed from the t - and P values derived from the group-level paired-samples t -test. Higher Z-scores represent greater pre-post intervention changes in functional connectivity between regions.

monitoring drug craving and mood measures throughout treatment; such data could be used as input to tailor this intervention. We also found pre-to post-session reductions in cortisol, a marker of HPA axis function [52]. Interestingly, prior treatment studies in chronic pain

patients have revealed parallel reductions in self-reported pain severity and cortisol levels [53]. Previous studies have also linked elevated cortisol levels with a higher rate of relapse among individuals with substance use disorders [54]. A study of this meditative intervention in

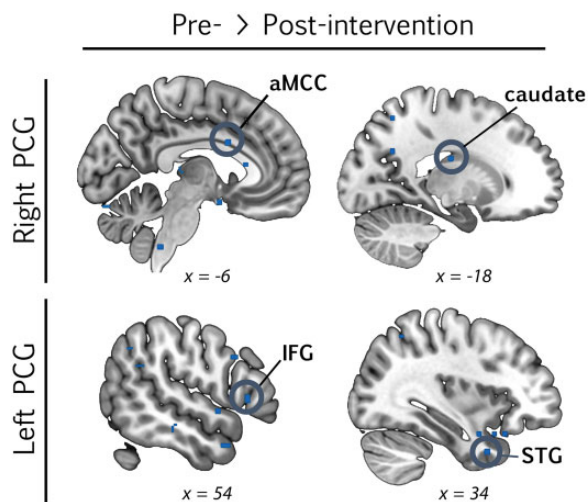


Figure 4. Reduced functional connectivity of the pain neuromatrix after the 12-week intervention (i.e., pre > post). Pain neuromatrix connectivity was estimated using seed-based resting-state functional connectivity of the left and right postcentral gyrus (PCG) with the rest of the brain. Image thresholded at $P < .01$ uncorrected for display purposes. Regions indicated with a circle reach the whole-brain corrected threshold for reduced (blue) strength of connectivity ($pFWE < 0.05$). See Table 2 for full list of significant results. aMCC = anterior middle cingulate cortex; IFG = inferior frontal gyrus; STG = superior temporal gyrus.

children with cancer found that post- (vs. pre-) session pain scores on a 0–10 VAS scale decreased among 85% of those who received the intervention, and 96% reported decreased post-session pain scores when pre-session scores were >5 ; furthermore, median pain scores decreased by 40%, more so for older than younger children [36]. Our working hypothesis is that this intervention may reduce pain and cortisol levels through active engagement of *intrinsic* and *extrinsic* cognition/affective processing, compared with more passive and self-focused interactions [55]. Specifically, this therapist-assisted VR intervention led the OUD patient to modify his/her own internal psychobiological state *and* to believe that his/her success in this regard was also helping others (i.e., children with cancer).

It is important to distinguish this meditative intervention from other modalities such as mindfulness and yoga. Whereas mindfulness uses intentional and non-judgmental conscious awareness of the present moment and yoga incorporates physical postures, breathing control, and meditation/relaxation, Martial Arts Therapy (while incorporating elements of both interventions) adds core concepts of “Power, Peace, and Purpose”. *Power* comes from introducing an expanded element controlling one’s situation. The mind-body movements coalesce to move the individual from passive acceptance of one’s predicament to active engagement toward change. *Peace* derives from acceptance of one’s current situation and can mitigate negative feelings that often create behavioral

stagnation. *Purpose* introduces elements of conviction and positive value for one’s existence and situation. It can help to transcend one’s situation and transform benign activity into something greater than the sum of its parts. Preliminary studies incorporating similar meditative interventions inspired by martial arts have shown promise in pain reduction [35, 36].

In addition to reductions in self-reported pain, there was a pre- to post-intervention reduction in pain task-related activation in the left PCG, a key region of the pain neuromatrix. Resting-state connectivity of the pain neuromatrix also changed from pre- to post-intervention, with reductions in connectivity between the PCG and other key regions (e.g., aMCC, caudate). The left PCG was the only pain neuromatrix ROI that significantly decreased in pain task-related activation from pre- to post-intervention. Left PCG activation was also positively correlated with baseline pain severity and cortisol levels. The PCG is a major part of the somatosensory cortex, implicated in perception of physical sensations from the body, including pain. The PCG is involved in anticipating and recognizing the location and intensity of pain [56], and may be involved in the development and/or maintenance of chronic pain [57].

Prior imaging studies have implicated the PCG in chronic pain and substance use disorders, including morphometric studies showing smaller PCG volume among polydrug users compared to non-users [58]. Smaller PCG volumes have also been reported in patients with chronic pain [59], and the PCG is consistently activated in fMRI studies of experimentally induced non-thermal pain [60]. Further, a study of individuals with cocaine use disorder found a decrease in PCG activity during a cognitive control task (i.e., Stroop) following a 12-week cognitive-behavioral therapy (CBT) and contingency management intervention [61]. In a follow-up study, greater pre- to post-CBT reductions in PCG activity were associated with longer duration of drug abstinence [8]. These findings suggest the PCG is relevant for both chronic pain and addiction, and may be treatment-responsive. A review of meditation interventions [10] suggested that meditation can attenuate pain ratings via reduced pain-related activation in the PCG, and experienced meditators show larger PCG gray matter volumes compared to less-experienced mediators. Results of the present study suggest a meditative intervention can reduce pain and modulate activity and connectivity of the PCG in OUD patients.

At baseline, the PCG showed positive connectivity with other regions of the pain neuromatrix, but this pattern changed post-treatment. In particular, PCG connectivity with the aMCC and caudate was lower post-intervention. The aMCC is associated with cognitive control of movement generation and emotional awareness, and encoding intensity of noxious pain [15]. The caudate is involved in planning movement execution and in sensing and suppressing pain [62, 63]. We also found higher

Table 3. Baseline pain severity and functional interference (Brief Pain Inventory) scores associated with resting-state functional connectivity of the postcentral gyrus (PCG) at pre- and post-intervention, and changes between pre- and post-intervention

Contrast Seed	Direction	Target Region	Brodmann Area	x	y	z	Cluster Extent	Z-score
Baseline pain severity associated with functional connectivity at baseline (i.e., pre-intervention)								
Left PCG	Higher pain severity, higher connectivity	Left cerebellum	N/A	-46	-64	-24	8	3.39
Right PCG	Higher pain severity, higher connectivity	Medial frontal gyrus	32	0	6	48	12	3.91
Left PCG	Higher pain severity, lower connectivity	Left precentral gyrus	4	-38	-24	-46	8	3.11
Right PCG	Higher pain severity, lower connectivity	Right superior frontal gyrus	6	20	8	54	8	3.14
Baseline pain functional interference associated with functional connectivity at baseline (i.e., pre-intervention)								
Left PCG	Higher pain interference, higher connectivity	No significant clusters						
Right PCG	Higher pain interference, higher connectivity	No significant clusters						
Left PCG	Higher pain interference, lower connectivity	No significant clusters						
Right PCG	Higher pain interference, lower connectivity	No significant clusters						
Baseline pain severity associated with functional connectivity at the post-intervention time point								
Left PCG	Higher pain severity, higher connectivity	Left inferior parietal lobe	1	-52	-26	44	10	3.44
Right PCG	Higher pain severity, higher connectivity	Right middle temporal gyrus	37	54	-64	0	12	3.66
Left PCG	Higher pain severity, lower connectivity	Left inferior parietal lobe	1	-46	-28	44	6	3.32
Right PCG	Higher pain severity, lower connectivity	Left occipital lobe	18	-32	-70	-6	8	3.10
Baseline pain functional interference associated with functional connectivity at the post-intervention time point								
Left PCG	Higher pain interference, higher connectivity	Left inferior parietal lobe	2	-52	-26	46	34	4.30
Right PCG	Higher pain interference, higher connectivity	Right inferior temporal lobe	20	44	-44	-18	20	4.00
Left PCG	Higher pain interference, lower connectivity	Left inferior parietal lobe	40	-64	-32	34	8	3.09
Right PCG	Higher pain interference, lower connectivity	Right precentral gyrus	6	40	-14	64	6	3.12
Baseline pain severity associated with changes in functional connectivity from pre- to post-intervention								
Left PCG	Higher pain severity, greater pre- to post reductions in connectivity	Right cerebellum (posterior lobe)	N/A	14	-58	-24	8	3.44
Right PCG	Higher pain severity, greater pre- to post reductions in connectivity	Left superior parietal lobe	7	-22	-52	48	6	3.45
		Right posterior cingulate cortex	23	8	-38	8	4	4.42
Left PCG	Higher pain severity, greater pre- to post increases in connectivity	Cerebellum (posterior lobe)	N/A	0	-70	-18	8	3.38
		Right precentral gyrus	6	40	-14	60	8	3.31
Right PCG	Higher pain severity, greater pre- to post increases in connectivity	Right middle frontal gyrus	11	20	40	-14	6	3.36
		Left hippocampus	N/A	-26	-18	-12	8	4.26
Left PCG	Higher pain interference, greater pre- to post reductions in connectivity	Left cerebellum	N/A	-18	-78	-52	8	3.09
		Left superior parietal lobe	7	-18	-60	48	8	3.39
		Left superior parietal lobe	7	-12	-64	64	8	3.37
Left PCG	Higher pain interference, greater pre- to post reductions in connectivity	Left superior parietal lobe	7	-24	-64	60	8	3.72

(continued)

Table 3. continued

Contrast Seed	Direction	Target Region	Brodmann Area	x	y	z	Cluster Extent	Z-score
Right PCG	Higher pain interference, greater pre- to post reductions in connectivity	No significant clusters						
Left PCG	Higher pain interference, greater pre- to post increases in connectivity	Right precentral gyrus	4	40	-18	60	10	4.41
Right PCG	Higher pain interference, greater pre- to post increases in connectivity	Right superior temporal gyrus	42	60	-32	14	8	3.47
		Left inferior parietal lobule.	40	-64	-24	34	12	3.27
		Left Brainstem	N/A	-14	-34	-58	11	3.32

All reported results are significant at the whole-brain corrected threshold (familywise error corrected using Monte Carlo simulations; voxel-wise threshold $P < .001$ and cluster-level correction (cluster minimum = 5 voxels). Cluster extent refers to the number of contiguous voxels in a cluster and the minimum cluster size was determined to be 5 voxels. Coordinates (x, y, z) refer to the anatomical location in 3D brain space, reported in MNI convention, at the peak maximally activated voxel within the cluster. Anatomical location of the peak location is reported using Brodmann areas. Note that separate target regions can have separate significant clusters within the same target region, particularly for anatomically large cortical regions. Test statistic given as a Z-score, which refers to the z statistic at the peak coordinate location. The Z-score was computed from the *t*- and *P* values derived from group-level regression analyses (BPI scores associated with functional connectivity or changes in functional connectivity). Higher Z-scores represent stronger connectivity between brain regions in those with higher BPI scores, or greater pre-post increases in connectivity in those with higher BPI scores. BPI = Brief Pain Inventory.

baseline cortisol levels were associated with greater post-treatment pain task-related insular activation. A primary role of the insula is pain perception including arousal and attention to nociceptive stimuli [20].

In addition to overall changes in PCG activation and connectivity, we found that baseline pain severity and interference scores were associated with changes in PCG connectivity from pre- to post-intervention. Patients with both higher pain severity and pain functional interference showed greater reductions in PCG–superior parietal lobe connectivity. The superior parietal lobe is involved in the perception and modulation of painful somatosensory sensations [64]. Furthermore, higher baseline pain severity was associated with less PCG–PCC connectivity. Previous studies have reported the PCC's possible role in modulating the conscious experience of pain [65]. Specifically, higher PCC activity has been associated with lower pain ratings [15]. Therefore, reduced PCG–PCC connectivity may indicate greater regulatory control of the PCC over sensory pain-related processing in the PCG either over time or due to the meditative intervention.

Our investigation should be interpreted in the context of limitations. This study was preliminary using a one-arm, unblinded design with a small sample. Thus, randomized controlled trials in larger samples are needed to evaluate efficacy of this intervention and to explore its mechanisms of effect. Also, the sample was predominantly female, which may relate to differences in pain perception and pain neuromatrix activity. Sex effects should be explored in future studies. Next, although all OUD patients were on MMT, it is unclear whether similar effects would be found for patients receiving other forms of OUD treatment. Furthermore, clinical

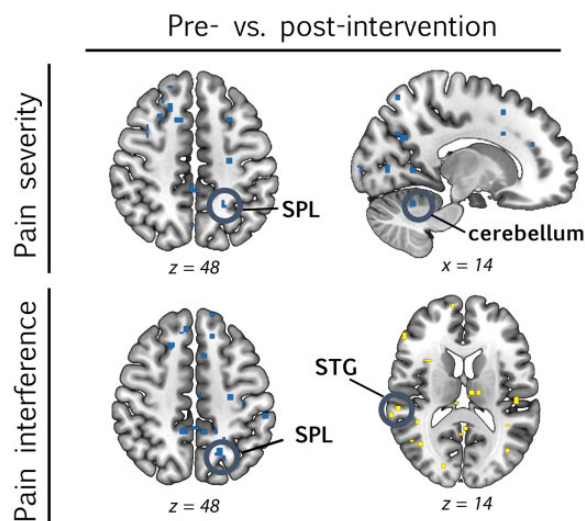


Figure 5. Pain severity and pain functional interference at baseline is associated with changes in connectivity of the pain neuromatrix from baseline to post-intervention. Higher pain severity (upper row) and pain functional interference (lower row) at baseline is associated with greater reductions (blue) or increases (yellow) in pain neuromatrix connectivity from pre- to post-intervention. Pain neuromatrix connectivity was estimated using seed-based resting-state functional connectivity of the left and right postcentral gyrus (PCG) with the rest of the brain. Image thresholded at $P < .01$ uncorrected for display purposes. Regions indicated with a circle reach the whole-brain corrected threshold for reduced (blue) or increased (yellow) strength of connectivity ($pFWE < 0.05$). See Table 3 for full list of significant results. SPL = superior parietal lobe; STG = superior temporal gyrus.

heterogeneity of the sample may have restricted our ability to observed changes over time in cortisol or CRP levels, and/or reported pain, anxiety, depression, and/or opioid craving.

The results of this feasibility study suggest a VR-based, meditative intervention is a promising approach for reducing pain ratings and modulating pain neuromatrix activity and connectivity among OUD patients. This intervention may be a beneficial part of a multidisciplinary pain and addiction management program.

The authors thank Kevin Browett (Kids Kicking Cancer) and Jared Welehodsky (MDHHS) for input during the planning phase; Joseph Urbiel for referral of participants; martial artists Richard Plowden, Peter Davenport, Autumm Heeter, and Joseph Genna for conducting the intervention; research assistants Alina Woodford, Hayley Harrison, and Lisa Sulkowski for session data collection and management; Klevis Karavidha for data extraction from participants' electronic medical records; Pavan Jella Kumar, Zahid Latif, and the WSU MR Research Facility for imaging data acquisition.

Authors' Contributions

M.M.F. and N.M.L. drafted key sections of the manuscript. A.M. is a martial artist who conducted some intervention sessions, and was involved in imaging data collection and analysis. E.G. and M.B. contributed to the study concept, development of the VR software, and supervised activities of the martial artists. H.A.M. conceptualized and supervised the brain imaging and data analyses, and edited the manuscript. M.K.G. conceptualized and designed the study, supervised all nonimaging data collection, management and analysis, and edited the manuscript.

Acknowledgements

Grants from Michigan Department of Health and Human Services (MDHHS no. E20182927-00) to Kids Kicking Cancer (E.G.) and NIH K01 MH119241 (to H.A.M.), the Gertrude Levin Endowed Chair in Addiction and Pain Biology (to M.K.G.), Helene Lycaki/Joe Young, Sr. Funds (MDHHS), and the Detroit Wayne Integrated Health Network supported this research. Funders were not involved in the conduct of the study, data analysis or interpretation, or decision to publish.

References

- Rudd RA, Seth P, David F, Scholl L. Increases in drug and opioid-involved overdose deaths—United States, 2010–2015. *MMWR Morb Mortal Wkly Rep* 2016;65(50–51):1445–52.
- Chen Q, Laroche MR, Weaver DT, et al. Prevention of prescription opioid misuse and projected overdose deaths in the United States. *JAMA Netw Open* 2019;2(2):e187621.
- Substance Abuse and Mental Health Services Administration. Key substance use and mental health indicators in the United States: Results from the 2018 National Survey on Drug Use and Health. HHS Publ No PEP19-5068, NSDUH Ser H-54 2019;170 :51–8.
- U.S. Department of Health and Human Services (HHS), Office of the Surgeon General. Facing Addiction in America: The Surgeon General's Spotlight on Opioids. Washington, DC: HHS; September 2018. Available at: https://addiction.surgeongeneral.gov/sites/default/files/Spotlight-on-Opioids_09192018.pdf
- Institute of Medicine (US) Committee on Advancing Pain Research, Care and Education. Relieving Pain in America: A Blueprint for Transforming Prevention, Care, Education, and Research. Washington, DC: National Academies Press; 2011. Available at: <https://pubmed.ncbi.nlm.nih.gov/22553896/>
- Hser YI, Mooney LJ, Saxon AJ, Miotto K, Bell DS, Huang D. Chronic pain among patients with opioid use disorder: Results from electronic health records data. *J Subst Abuse Treat* 2017;77 :26–30.
- Vest NA, McPherson S, Burns GL, Tragesser S. Parallel modeling of pain and depression in prediction of relapse during buprenorphine and naloxone treatment: A finite mixture model. *Drug Alcohol Depend* 2020;209:107940.
- Moningka H, Lichenstein S, Worhunsky PD, DeVito EE, Scheinost D, Yip SW. Can neuroimaging help combat the opioid epidemic? A systematic review of clinical and pharmacological challenge fMRI studies with recommendations for future research. *Neuropsychopharmacology* 2019;44(2):259–73.
- Boscarino JA, Rukstalis MR, Hoffman SN, et al. Prevalence of prescription opioid-use disorder among chronic pain patients: Comparison of the DSM-5 vs. DSM-4 diagnostic criteria. *J Addict Dis* 2011;30(3):185–94.
- Khusid MA, Vythilingam M. The emerging role of mindfulness meditation as effective self-management strategy, part 2: Clinical implications for chronic pain, substance misuse, and insomnia. *Mil Med* 2016;181(9):969–75.
- Wells RE, Collier J, Posey G, et al. Attention to breath sensations does not engage endogenous opioids to reduce pain. *Pain* 2020; 161(8):1884–93.
- Zeidan F, Martucci KT, Kraft RA, Gordon NS, McHaffie JG, Coghill RC. Brain mechanisms supporting the modulation of pain by mindfulness meditation. *J Neurosci* 2011;31 (14):5540–8.
- Morone NE, Lynch CS, Greco CM, Tindle HA, Weiner DK. "I felt like a new person." The effects of mindfulness meditation on older adults with chronic pain: Qualitative narrative analysis of diary entries. *J Pain* 2008;9(9):841–8.
- Garland EL, Thomas E, Howard MO. Mindfulness-oriented recovery enhancement ameliorates the impact of pain on self-reported psychological and physical function among opioid-using chronic pain patients. *J Pain Symptom Manage* 2014;48 (6):1091–9.
- Reddan MC, Wager TD. Modeling pain using fMRI: From regions to biomarkers. *Neurosci Bull* 2018;34(1):208–15.
- Ochsner KN, Silvers JA, Buhle JT. Review and evolving model of the cognitive control of emotion. *Ann NY Acad Sci* 2012;1251 (1):E1–24.
- Bunney PE, Zink AN, Holm AA, Billington CJ, Kotz CM. Orexin activation counteracts decreases in nonexercise activity thermogenesis (NEAT) caused by high-fat diet. *Physiol Behav* 2017;176(1):139–48.
- Iannetti GD, Mouraux A. From the neuromatrix to the pain matrix (and back) [Internet]. In: *Experimental Brain Research*. Vol. 205. Springer Verlag; 2010: 1–12. Available at: <https://pubmed.ncbi.nlm.nih.gov/20607220/> (accessed January 31, 2021).

19. Jacoby N, Bruneau E, Koster-Hale J, Saxe R. Localizing Pain Matrix and Theory of Mind networks with both verbal and non-verbal stimuli. *Neuroimage* 2016;126:39–48.
20. Nakata H, Sakamoto K, Kakigi R. Meditation reduces pain-related neural activity in the anterior cingulate cortex, insula, secondary somatosensory cortex, and thalamus. *Front Psychol* 2014;5.
21. Grant JA, Courtemanche J, Rainville P. A non-elaborative mental stance and decoupling of executive and pain-related cortices predicts low pain sensitivity in Zen meditators. *Pain* 2011;152(1):150–6.
22. Grant JA, Rainville P. Pain sensitivity and analgesic effects of mindful states in Zen meditators: A cross-sectional study. *Psychosom Med* 2009;71(1):106–14.
23. Cleeland C. Brief Pain Inventory User Guide; 2009. Available at: https://www.mdanderson.org/documents/Departments-and-Divisions/Symptom-Research/BPI_UserGuide.pdf
24. Naji L, Dennis BB, Bawor M, Plater C, et al. A prospective study to investigate predictors of relapse among patients with opioid use disorder treated with methadone. *Subst Abuse Res Treat* 2016;10:9–18.
25. Beck AT, Steer RA, Brown G. Manual for the Beck Depression Inventory-II. San Antonio, TX: Psychological Corporation; 1996.
26. Buckley TC, Parker JD, Heggie J. A psychometric evaluation of the BDI-II in treatment-seeking substance abusers. *J Subst Abuse Treat* 2001;20(3):197–204.
27. Spielberg CD, Gorsuch RL, Lushene R, Vagg P, Jacobs GA. Manual for the State-Trait Anxiety Inventory. Palo Alto, CA: Consulting Psychologists Press; 1970.
28. Simons JS, Gaher RM. The distress tolerance scale: Development and validation of a self-report measure. *Motiv Emot* 2005;29(2):83–102.
29. Brown RA, Lejuez CW, Kahler CW, Strong DR. Distress tolerance and duration of past smoking cessation attempts. *J Abnorm Psychol* 2002;111(1):180–5.
30. Daughters SB, Lejuez CW, Kahler CW, Strong DR, Brown RA. Psychological distress tolerance and duration of most recent abstinence attempt among residential treatment-seeking substance abusers. *Psychol Addict Behav* 2005;19(2):208–11.
31. Cohen S. Perceived Stress Scale (PSS). *Encycl Behav Med* 1994:1–5.
32. Gratz KL, Roemer L. Difficulties in Emotion Regulation Scale (DERS). *J Psychopathol Behav Assess* 2004;26(1):41–54.
33. Brown TG, Seraganian P, Tremblay J, Annis H. Process and outcome changes with relapse prevention versus 12-step aftercare programs for substance abusers. *Addiction* 2002;97(6):677–89.
34. Zeidan F, Vago DR. Mindfulness meditation-based pain relief: A mechanistic account. *Ann N Y Acad Sci* 2016.
35. Marusak HA, Cohen C, Goldberg E, et al. Martial arts-based therapy reduces pain and distress among children with chronic health conditions and their siblings. *J Pain Res* 2020;13:3467–78.
36. Bluth MH, Thomas R, Cohen C, Bluth AC, Goldberg E. Martial arts intervention decreases pain scores in children with malignancy. *Pediatric Health Med Ther* 2016;7:79–87.
37. Baler RD, Volkow ND. Drug addiction: The neurobiology of disrupted self-control. *Trends Mol Med* 2006;12(12):559–66.
38. Gerritsen RJS, Band GPH. Breath of life: The respiratory vagal stimulation model of contemplative activity. *Front Hum Neurosci* 2018;12.
39. Frangos E, Richards EA, Bushnell MC. Do the psychological effects of vagus nerve stimulation partially mediate vagal pain modulation? *Neurobiol Pain* 2017;1:37–45.
40. Kundu P, Brenowitz ND, Voon V, et al. Integrated strategy for improving functional connectivity mapping using multiecho fMRI. *Proc Natl Acad Sci USA* 2013;110(40):16187–92.
41. Lombardo MV, Auyeung B, Holt RJ, et al. Improving effect size estimation and statistical power with multi-echo fMRI and its impact on understanding the neural systems supporting mentalizing. *Neuroimage* 2016;142:55–66.
42. Power JD, Mitra A, Laumann TO, Snyder AZ, Schlaggar BL, Petersen SE. Methods to detect, characterize, and remove motion artifact in resting state fMRI. *Neuroimage* 2014;84:320–41.
43. Woo CW, Krishnan A, Wager TD. Cluster-extent based thresholding in fMRI analyses: Pitfalls and recommendations. *Neuroimage* 2014;91:412–9.
44. Cox RW, Chen G, Glen DR, Reynolds RC, Taylor PA. FMRI clustering in AFNI: False-positive rates redux. *Brain Connect* 2017;7(3):152–71.
45. Smith SM, Fox PT, Miller KL, et al. Correspondence of the brain's functional architecture during activation and rest. *Proc Natl Acad Sci USA* 2009;106(31):13040–5.
46. Cole MW, Bassett DS, Power JD, Braver TS, Petersen SE. Intrinsic and task-evoked network architectures of the human brain. *Neuron* 2014;83(1):238–51.
47. Moeller S, Nallasamy N, Tsao DY, Freiwald WA. Functional connectivity of the macaque brain across stimulus and arousal states. *J Neurosci* 2009;29(18):5897–909.
48. Spisak T, Kincses B, Schlitt F, et al. Pain-free resting-state functional brain connectivity predicts individual pain sensitivity. *Nat Commun* 2020;11(1):1–12.
49. Flodin P, Martinsen S, Altawil R, et al. Intrinsic brain connectivity in chronic pain: A resting-state fMRI study in patients with rheumatoid arthritis. *Front Hum Neurosci* 2016;10:107.
50. Kieliba P, Madugula S, Filippini N, Duff EP, Makin TR. Large-scale intrinsic connectivity is consistent across varying task demands. *PLoS One* 2019;14(4).
51. Whitfield-Gabrieli S, Nieto-Castanon A. Conn: A functional connectivity toolbox for correlated and anticorrelated brain networks. *Brain Connect* 2012;2(3):125–41.
52. Hellhammer DH, Wüst S, Kudielka BM. Salivary cortisol as a biomarker in stress research. *Psychoneuroendocrinology* 2009;34(2):163–71.
53. Evans KD, Douglas B, Bruce N, Drummond PD. An exploratory study of changes in salivary cortisol, depression, and pain intensity after treatment for chronic pain. *Pain Med* 2008;9(6):752–8.
54. Milivojevic V, Sinha R. Central and peripheral biomarkers of stress response for addiction risk and relapse vulnerability. *Trends Mol Med* 2018;24(2):173–86.
55. Hede A. Binary model of the dynamics of active versus passive mindfulness in managing depression. *OBM Integr Complement Med* 2018;3(4):1.
56. Vierck CJ, Whitsel BL, Favorov OV, Brown AW, Tommerdahl M. Role of primary somatosensory cortex in the coding of pain. *Pain* 2013;154(3):334–44.
57. Kim W, Kim SK, Nabekura J. Functional and structural plasticity in the primary somatosensory cortex associated with chronic pain. *J Neurochem* 2017;141(4):499–506.
58. Noyan CO, Kose S, Nurmedov S, Metin B, Darcin AE, Dilbaz N. Volumetric brain abnormalities in polysubstance use disorder patients. *Neuropsychiatr Dis Treat* 2016;12:1355–63.
59. Schmidt-Wilcke T, Leinisch E, Gänßbauer S, et al. Affective components and intensity of pain correlate with structural differences in gray matter in chronic back pain patients. *Pain* 2006;125(1–2):89–97.
60. Friebe U, Eickhoff SB, Lotze M. Coordinate-based meta-analysis of experimentally induced and chronic persistent neuropathic pain. *Neuroimage* 2011;58(4):1070–80.

61. Devito EE, Dong G, Kober H, Xu J, Carroll KM, Potenza MN. Functional neural changes following behavioral therapies and disulfiram for cocaine dependence. *Psychol Addict Behav* 2017;31(5):534–47.
62. Wunderlich AP, Klug R, Stuber G, Landwehrmeyer B, Weber F, Freund W. Caudate nucleus and insular activation during a pain suppression paradigm comparing thermal and electrical stimulation. *Open Neuroimag J* 2011;5:1–8.
63. Grahn JA, Parkinson JA, Owen AM. The cognitive functions of the caudate nucleus. *Prog Neurobiol* 2008;86(3):141–55.
64. Duncan GH, Albanese MC. Is there a role for the parietal lobes in the perception of pain? *Adv Neurol* 2003;93:69–86.
65. Fauchon C, Faillenot I, Quesada C, et al. Brain activity sustaining the modulation of pain by empathetic comments. *Sci Rep* 2019;9(1):1–10.